TRANSMUTATION OF LONG-LIVED FISSION PRODUCTS IN A SODIUM-COOLED ATW SYSTEM

Y. Kim,[1] **R.N. Hill, W-S. Yang** and **H. Khalil**
Argonne National Laboratory
9700 S. Cass Avenue, Argonne, Illinois 60439-4842, USA

Abstract

To devise an optimal strategy for transmuting long-lived fission products (LLFPs) in fast systems, various design studies have been performed for a sodium-cooled Accelerator Transmutation of Waste system. For ^{99}Tc and ^{129}I target assemblies loaded with metallic ^{99}Tc and CaI_2 targets and ZrH_2 moderator, assembly design studies were first performed, focused on the optimisation of neutron spectrum and the reduction of local power peaking in neighbouring fuel assemblies caused by moderation in the target assembly. Then, using optimised LLFP target assembly designs, full core depletion calculations were carried out to find optimum loading options. The result shows that loading of moderated target assemblies in the core periphery (reflector region) is preferable from the viewpoint of neutron economy and safety. By a simultaneous loading of twelve ^{99}Tc and twelve ^{129}I target assemblies in the reflector region, ^{99}Tc and ^{129}I are consumed with a support ratio equal to the transuranic support ratio (~3.2) at the cost of a 10% increase in fuel inventory. Consumption fractions of ~29% and ~37% are achieved at discharge for ^{99}Tc and ^{129}I target assemblies with a ~5-year irradiation period.

1. Korea Atomic Energy Research Institute, Republic of Korea.

I. Introduction

If the transuranic (TRU) inventory is reduced significantly by deploying TRU transmuters, the long-lived fission products (LLFPs) will likely dominate the long-term dose associated with radionuclide release from the geological repository. To reduce the long-term dose, it has been suggested to transmute LLFPS into short-lived isotopes by neutron capture, and various studies of the LLFP transmutation in reactor systems have previously been performed. [1-8] Among these LLFPs, ^{99}Tc, ^{129}I, and ^{135}Cs are the most problematic isotopes in terms of the collective leakage-dose risk (which increases with toxicity and mobility) in the repository. However, only ^{99}Tc and ^{129}I are generally considered practical to transmute in reactor systems, since the effective transmutation of ^{135}Cs requires isotopic separation and very high neutron flux even in a thermal spectrum.

Even though capture cross sections are higher in thermal systems than in fast systems, efficient transmutation of ^{99}Tc and ^{129}I in thermal reactors such as current LWRs would be difficult and expensive because of the impracticably low transmutation rate and the large inventories required, which result from the comparatively low flux level. [1] Fast systems are more attractive because of the surplus neutrons that could be used for target transmutation. They also provide more flexibility for LLFP loading. To take advantage of higher capture cross sections for thermal neutrons, the neutron spectrum in LLFP target assemblies can also be moderated by employing metal hydrides such as ZrH_2 and CaH_2. [1-5] These moderated target assemblies can be positioned in the inner core to take full advantage of the higher flux level of fast systems. (However, it requires additional design measures to reduce the local power peaking in nearby fuel pins caused by moderation in the target assembly.) Alternatively, neutron leakage from a fast reactor core can be utilised more efficiently by locating LLFP target assemblies at the core periphery (e.g., in the reflector region).

Several target material forms for ^{99}Tc and ^{129}I transmutation have been studied. Typically, metallic targets have been proposed for ^{99}Tc transmutation and iodide forms (NaI, CaI_2, CeI_3, PbI_2, etc.) have been considered for ^{129}I. Technetium can also be loaded "homogeneously" by commingling it with the fuel, unlike iodine which is difficult to mix with the fuel. Irradiation tests performed in the High Flux Reactor at Petten concluded that there is no technical limitation to the use of metallic technetium and that sodium iodide seems to be the best candidate among the three target iodine forms (NaI, CeI_3, and PbI_2) from the point of view of compatibility with 15-15 titanium stainless steel cladding and with reprocessing technology. [6-8] It has also been reported that a sodium iodide (NaI) and a calcium iodide (CaI_2) are desirable target forms for ^{129}I in terms of their chemical characteristics. [8] To avoid the expense of isotopic separation, the iodide target is directly formed with the elemental iodine extracted from the spent nuclear fuel, which includes both ^{129}I and ^{127}I fission products.

To devise an optimal strategy for transmuting LLFPs in fast systems, design optimisation studies were performed for an 840 MW-thermal sodium-cooled Accelerator Transmutation of Waste (ATW) system. [9] Using metallic ^{99}Tc and CaI_2 target forms and ZrH_2 moderator, assembly design optimisation studies were first done to maximise the LLFP transmutation performance and to mitigate the local power peaking problem in neighbouring fuel assemblies caused by moderation in the target assembly. Then, using optimised LLFP target assembly designs, full core depletion calculations were carried out for various target loading options including the loading of moderated target assemblies in the inner core and the reflector region and the homogeneous mixing of LLFP with fuel. For simultaneous loading of ^{99}Tc and ^{129}I target assemblies, further assembly design optimisation was performed to equalise the ^{99}Tc and ^{129}I support ratios to the TRU support ratio, assuring that neither the long-lived TRUs nor LLFPs accumulate.

The results of these optimisation studies are presented in this paper. In Section II, the methods and results of the assembly design optimisation studies are presented. The LLFP loading option studies are discussed in Section III along with the LLFP transmutation results and system performance impacts. Conclusions are presented in Section IV.

II. LLFP Target assembly design studies

In the case of repeated recycle, the loss rate of LLFPs to the repository is basically determined by the discharge burn-up (i.e., the fractional consumption at discharge) and the recovery factor per recycle pass. The loss rate monotonically decreases as desired as the discharge burn-up and recovery factor increase. The (currently targeted) recovery factor for LLFP elements is about 95%, while it is over 99.9% for TRU elements. Considering this relatively low recovery factor, the discharge burn-up of LLFP target assemblies should be maximised under various design and operation constraints.

For fixed total flux level and residence time, the LLFP discharge burn-up is primarily determined by the effective one-group capture cross sections. To take advantage of higher LLFP capture cross sections for thermal neutrons, the LLFP target assemblies are generally moderated with metal hydrides such as ZrH_2 and CaH_2. In a moderated LLFP target assembly, as the moderator loading fraction increases, the effective capture cross section (i.e., relative transmutation rate) increases due to the enhanced moderation and reduced self-shielding effects of LLFP isotopes. On the other hand, the increase of moderator loading fraction results in a reduced LLFP loading and hence a reduced absolute transmutation rate. As a result, it is expected that there exists an optimum moderator loading fraction which provides a good compromise between the goals of maximising both the relative and absolute LLFP transmutation rates.

Figure 1. **LLFP Assembly configuration and seven-assembly VIM computational model**

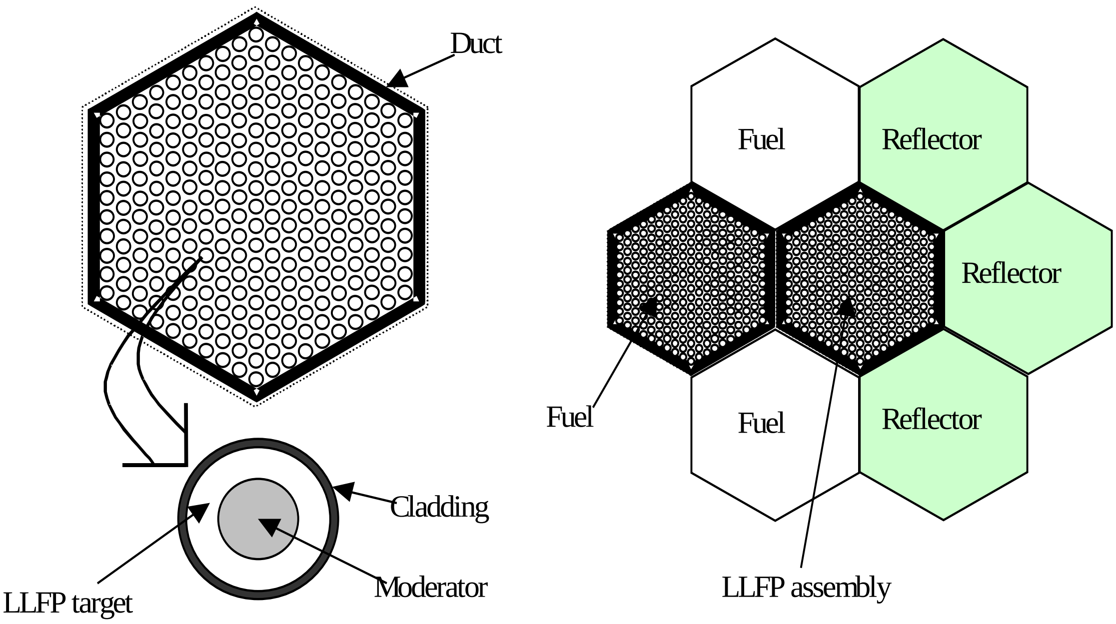

a) Configuration of LLFP assembly

b) VIM model for reflector zone loading

Spectral optimisation studies were first performed for moderated ^{99}Tc and ^{129}I target assemblies. To account for the local heterogeneity effects, calculations were carried out with the VIM continuous Monte Carlo code. [10] Then, various thermal neutron filter concepts were examined to reduce the local power peaking in neighbouring fuel assemblies caused by target moderation

II.1 Spectral optimisation

For spectral optimisation studies, a reference target assembly design was developed based on previous studies and preliminary analyses. In this design, target pins composed of annular technetium or iodine target material surrounding ZrH_2 moderator within a HT-9 cladding are arranged in a triangular array inside a HT-9 hexagonal duct, as shown in Figure 1a. Table 1 summarises the assembly design parameters which were selected in part to be compatible with the ATW fuel assembly design. [9] Metallic technetium was assumed for the ^{99}Tc target. As the iodine target material, CaI_2 compound was selected because of relatively high melting points of CaI_2 (783°C) and calcium (842°C). (NaI is expected to melt when the sodium is liberated from iodine due to the transmutation, and this might be a problem for achieving a high discharge burn-up.) Isotopic separation of ^{129}I was excluded, and an iodine vector of 77% ^{129}I and 23% ^{127}I (typical of PWR spent fuel isotopic ratio) was used for the iodine target.

Table 1. **Design parameters of reference LLFP target assembly**

Number of target pins per assembly	271
Pin diameter, cm	0.74422
Cladding thickness, cm	0.05588
Pitch-to-diameter (P/D) ratio	1.1969
Active length, cm	106.68
Duct outside flat-to-flat, cm	15.7099
Duct wall thickness, cm	0.3937
Interassembly gap, cm	0.4318
Assembly pitch, cm	16.1417

For this reference assembly design, the optimum moderator fraction was first sought for each of the technetium and iodine target assemblies by adjusting the moderator volume fraction inside the cladding. For a given moderator volume fraction, two variations of target configuration were also investigated: cylindrical target surrounded by annular moderator and homogeneous mixture of LLFP target and moderator. To account for local heterogeneity effects, Monte Carlo calculations were performed with VIM. In order to examine the spectral and LLFP resonance self-shielding effects without introducing excessive computational burden, two seven-assembly models were developed for target assembly loadings in the inner core and reflector regions; an LLFP target assembly is surrounded by six fuel assemblies in the model for the inner core loading, but it is surrounded by three fuel assemblies and three HT-9 reflector assemblies in the model for the reflector region loading as shown in Figure 1b. The fuel assembly was loaded with a Zr-based TRU fuel, and the TRU isotopic vector of LWR spent nuclear fuel was used. In both models, one of the fuel assemblies was evaluated in detail to assess the local power peaking due to the thermal neutron leakage from the LLFP assembly. With the reflective boundary conditions imposed, the VIM calculations were performed with the ENDF/B-V cross section library at 300°K.

Using these seven-assembly computational models, Monte Carlo VIM calculations were carried out for various moderator volume fractions by adjusting the target thickness. In order to separate out the spectrum softening effects, the VIM calculation for each target thickness was repeated by setting moderator density to zero. The results are summarised in Tables 2 and 3, and in Figures 2 to 4. Table 2 shows the effective one-group capture cross sections of ^{99}Tc, ^{127}I, and ^{129}I along with the power peaking factor in the fuel assembly. The results show that the capture cross sections of the three isotopes monotonically increase as the moderator volume increases. This is due to the reduced resonance self-shielding and the softened neutron spectrum. Even in the zero moderator density case, the capture cross section increases as the target thickness decreases due to the reduced spatial self-shielding effects. Compared to ^{99}Tc, ^{129}I shows a substantially larger increase of the effective capture cross mainly because of its higher thermal capture cross section. The increase of the ^{99}Tc cross section is largely due to the reduced self-shielding of the large resonance peak at 5.6eV. (The resonance integral is ~340 barns for ^{99}Tc, while it is ~36 barns for ^{129}I.) These energy effects are illustrated in Figure 2 which shows the normalised capture reaction rate distributions over a 27-group structure for a 60% moderator volume. The thermal group reaction rate is much larger than those of other groups in the ^{129}I target. For the ^{99}Tc target, the thermal reaction rate is slightly larger than that of the 24th group, which contains a large resonance. In the case of inner core loading, the capture cross sections are slightly reduced relative to the reflector loading case due to harder neutron spectrum.

Figure 2. **Group-wise capture reaction rate in LLFP assemblies with a 60% moderator volume**

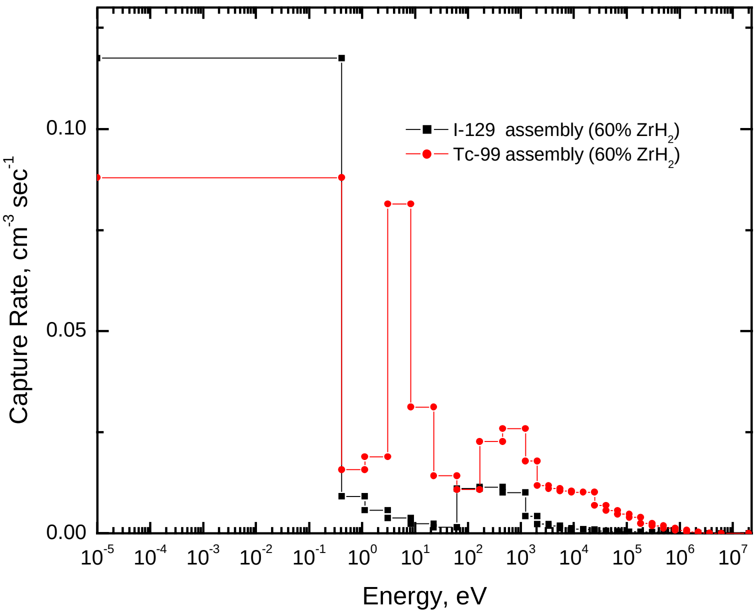

As shown in Table 2, the ZrH_2 moderator in the LLFP target assembly induces a large local power peaking in the adjacent fuel assemblies. The power peaking problem is more pronounced in the iodine target assembly case. This is mainly due to the larger mean free path of thermal neutrons in CaI_2 than in technetium; the thermal neutron mean path is about three times larger in CaI_2 than in technetium since the iodine atom density in CaI_2 target is ~3.8 times smaller than the ^{99}Tc atom density in metallic technetium target. The extra neutron moderation by the calcium nuclides contributes additionally. Compared to the reflector loading case, the power peaking of the inner core loading case is increased considerably for the ^{129}I target assembly, but marginally for the ^{99}Tc target assembly.

Table 2. **Moderator effects on effective capture cross sections and power peaking**

ZrH_2 volume fraction	^{99}Tc target		CaI$_2$ target		
	One-group capture cross section of ^{99}Tc, barn	Power peaking factor in fuel assembly	One-group capture cross section of ^{127}I, barn	One-group capture cross section of ^{129}I, barn	Power peaking factor in fuel assembly
LLFP target loading in reflector region					
0.0	0.43 (0.43[1)])	1.09	0.71 (0.71[1)])	0.37 (0.37[1)])	1.07
0.2	0.78 (0.49)	1.08	2.19 (0.83)	1.20 (0.43)	1.54
0.4	1.23 (0.57)	1.28	3.00 (0.99)	2.11 (0.51)	2.14
0.6	1.94 (0.70)	1.64	3.70 (1.24)	3.31 (0.61)	2.74
0.8	3.39 (0.91)	2.22	4.52 (1.71)	4.98 (0.79)	3.32
0.9	4.99 (1.12)	2.81	5.18 (2.12)	6.11 (0.92)	3.67
LLFP target loading in inner core					
0.6	1.84	1.87	3.54	3.10	3.44

1) Zero moderator density case.

In Figures 3 and 4, the capture reaction rates and relative transmutation rates normalised to the un-moderated case are plotted as a function of the moderator volume fraction. It can be observed that a moderator fraction at the vicinity of 0.4 provides the maximum capture rate, that is, the maximum absolute transmutation rate (LLFP mass transmuted per unit time). With this optimal moderator volume fraction, the capture rate is increased by about 15% for ^{99}Tc and by about 150% for ^{129}I relative to the un-moderated case. The ^{129}I capture rate is increased much more significantly by moderation since the capture cross section of ^{129}I is more efficiently enhanced by the ZrH_2 moderator due to its higher thermal cross section. Comparing the capture rates of the normal and zero moderator cases, most of these capture rate increases can be ascribed to the moderator. These results show that a desired absolute transmutation rate can be achieved with a much smaller LLFP loading by employing the moderator. For a fixed amount of LLFP loading per target assembly, the maximum transmutation performance is achieved by arranging the LLFP target pins in such a way that the moderator volume is maximised. This suggests that total volume for the target and moderator should be maximised subject to assembly thermal design constraints.

Figures 3 and 4 also show that the relative transmutation rate (fraction of LLFP transmuted per a unit time) increases monotonically with the moderator volume fraction. As a result, the LLFP loading needs to be minimised in order obtain the maximum target discharge burn-up, which is desired to reduce the LLFP loss to the repository. On the other hand, in order to maximise the LLFP incineration, the moderator volume fraction needs to be selected at the vicinity of 0.4 as discussed above; in the region of moderator volume fraction above 0.4, the absolute transmutation rate decreases monotonically with the moderator volume fraction. Furthermore, the power peaking in nearby fuel assemblies also increases monotonically as the moderator volume fraction in the target assembly increases. Considering these three conflicting performance indices, it is believed that a moderator volume fraction of 0.6~0.7 is a good compromise.

Figure 3. **^{99}Tc Transmutation rates versus moderator volume fraction**
(reflector loading case)

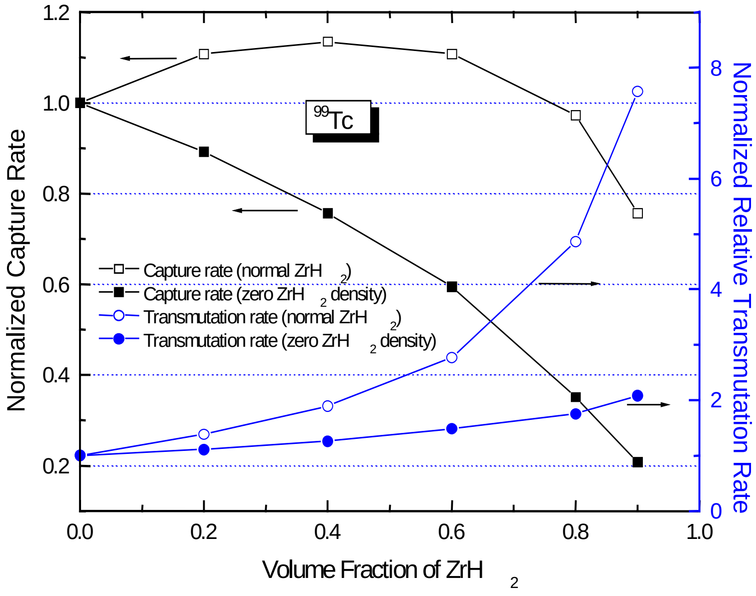

Figure 4. **^{129}I Transmutation rates versus moderator volume fraction**
(reflector loading case)

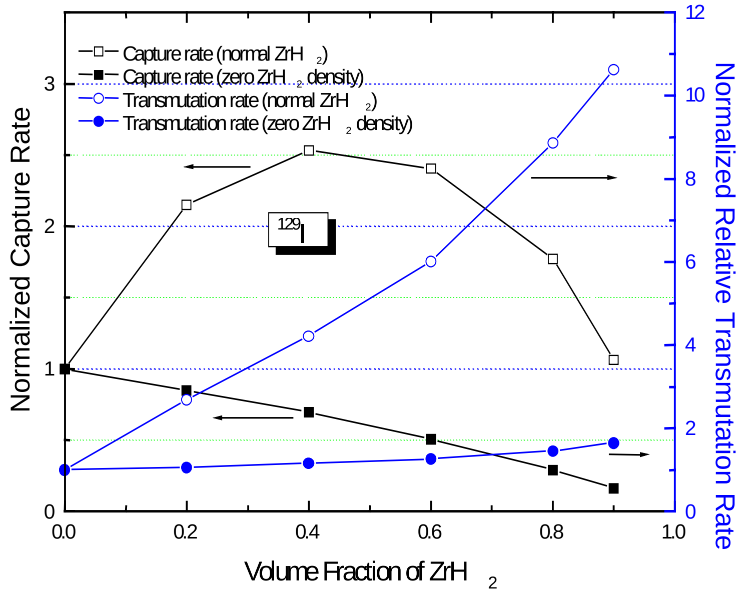

For the 60% moderator volume fraction, two variations of target configuration were also investigated: 1) central cylindrical target surrounded by annular moderator and 2) homogeneous mixture of LLFP target and moderator. The effective one-group capture cross sections are compared in Table 3. In terms of the relative transmutation rate, the homogeneous mixture provides the best performance (due to the minimised self-shielding effect) increasing the rate by about 5% and the central cylindrical target gives the worst performance, but the differences are small. Furthermore, the power peaking problem is exacerbated in the homogeneous mixture and the annular moderator options. In addition, it is not clear at this moment whether the homogeneous mixing concept is technically feasible from the fabrication/irradiation point of view.

For the same moderator volume fraction in the LLFP target assembly, these target designs generally provide larger LLFP capture cross sections due to the reduced self-shielding effects, compared to previous studies [2,5] where distinct LLFP target and moderator pins are employed either with a uniform pin diameter or with an irregular pin diameter (larger moderator pin diameter). Therefore, in terms of the effective LLFP capture cross sections, the LLFP target assembly based on the annular target concept could be considered as a near-optimal design. However, the material compatibility between LLFP targets and ZrH_2 moderator needs to be established, although no serious compatibility issue is expected.

II.2 Thermal neutron filter

As discussed in the previous subsection, the moderated LLFP target assembly substantially enhances the LLFP transmutation rates. On the other hand, the moderation in the target assembly also results in an increased local power peaking in the nearby fuel assemblies. To mitigate the power peaking, a thicker duct wall has been proposed. [2] However, this option is not attractive from the neutron utilisation viewpoint. To reduce the thermal neutron leakage from the LLFP assembly to the neighbouring fuel assemblies, a ^{99}Tc plate could be placed between the duct wall and the target pins. [5] This latter scheme has an advantage that the leaking thermal neutrons can be utilised to transmute ^{99}Tc thermal neutron filter, although its transmutation rate is relatively lower compared to the interior targets. In this work, a variant of the latter option was examined by replacing the target pins in the outer rings with un-moderated ^{99}Tc pins along the boundary between the LLFP and fuel assemblies. For the ^{129}I target assembly, the CaI_2 target pins in two outer rings were replaced with cylindrical ^{99}Tc target pins. In the case of the ^{99}Tc target assembly, the internal moderator was removed from the target pins in the outermost ring.

Using the seven-assembly VIM model for the reflector loading case, the effects of the ^{99}Tc thermal neutron filter were investigated for ^{99}Tc and ^{129}I target assemblies. For comparison, each calculation was repeated by replacing the ^{99}Tc pins with HT-9 pins. The resulting local power peaking factors are presented in Table 4. By employing the un-moderated ^{99}Tc pins as the thermal neutron filter, the initial local power peaking factor was reduced from 1.64 to 1.43 for the ^{99}Tc target assembly and from 2.74 to 1.40 for the ^{129}I target assembly. On the other hand, the effective capture cross sections were slightly reduced because of reduced moderation, as expected. The results also show that HT-9 pins are not as efficient as ^{99}Tc pins as the thermal neutron filter, especially for the ^{129}I target assembly; for sufficient filtering of thermal neutrons, more ^{129}I target pins needs to be replaced by the HT-9 pins, which would reduce the ^{129}I transmutation performance.

Table 4. Local power peaking of fuel assembly neighbouring to LLEP target assembly with thermal neutron filter (60% moderator volume fraction)

LLFP burn-up (atom %)	**Power peaking in neighboring fuel assembly**	
	^{99}Tc target	CaI_2 target
0	1.43 (1.49*)	1.40 (2.04*)
40	1.46	1.55

* HT-9 rods are used instead of ^{99}Tc as the thermal neutron filter.

By neutron capture, technetium and iodine isotopes are converted mainly into ^{100}Ru and ^{130}Xe, respectively. Since the capture cross sections of these product isotopes are significantly smaller than those of target isotopes, the power peaking is likely to increase with target burn-up. Therefore, the power peaking factors were estimated for a 40 a/o burn-up of ^{99}Tc, ^{127}I and ^{129}I. To get a conservative estimate, it was assumed that ^{127}I and ^{129}I are converted into void and ^{99}Tc is converted into ^{101}Ru, which has a slightly smaller thermal capture cross section than ^{100}Ru. As shown in Table 4, the high LLFP burn-up increases the power peaking slightly. However, this power peaking increase is considered tolerable based on the conservative peaking factor evaluation.

The power peaking factors presented in Table 4 provide generally conservative values for the LLFP assembly loading in the reflector region, since the reflective boundary condition was imposed on the boundary. In the actual configuration, a steep flux gradient exists across the fuel, target, and reflector assemblies, and this is expected to reduce the power peaking in the fuel assembly. In addition, in the LWR spent fuel TRU used in these calculations, ^{239}Pu fraction is comparatively high (more than 50%), and resulting in a high power peaking factor. In an equilibrium core, the ^{239}Pu fraction would be significantly lower, helping reduce the power peaking. Furthermore, the assembly power density in the core periphery is generally low. Therefore, it is likely that the power peaking factors shown in Table 4 would be tolerable, although more detailed analyses need to be performed for a specific application. On the other hand, the power peaking needs to be reduced further when LLFP target assemblies are loaded in the inner core.

III. LLFP transmutation performance of an ATW system

Using the LLFP target assembly designs discussed in the previous section, the ^{99}Tc and ^{129}I transmutation capability of an ATW system [9] was investigated by performing full core depletion calculations for various target loading options including the moderated target assembly loading in the inner core and in reflector regions and a homogeneous mixing of LLFP with fuel. ATW system design parameters are based on the studies in Reference 9. For simultaneous loading of ^{99}Tc and ^{129}I target assemblies, further assembly design optimisation was performed to equalise the ^{99}Tc and ^{129}I support ratios to the TRU fuel support ratio.

The full core depletion calculations were performed with the REBUS-3 code system. [11] The flux calculations were performed with triangular-Z models using the finite difference diffusion theory option. The region-dependent 27-group cross sections were generated using the MC^2-2 code [12] based on ENDF/B-V data. Since MC^2-2 is not designed to generate the thermal group data, the thermal group (E <0.414 eV) cross sections for the moderated LLFP target assemblies were estimated for the seven-assembly models described in the previous section using the VIM code based on the ENDF/B-V library.

III.1 LLFP transmutation objectives

The main design objective of the sodium-cooled ATW system is to consume TRU as efficiently as possible. To limit the burn-up reactivity swing, a half-year cycle (135 effective full power days, EFPD) is adopted. The charged fuel contains the TRUs recovered via recycle from the discharged ATW fuel, supplemented by LWR-discharge TRU to make up for the TRU consumed by fission. During recycle and re-fabrication, it is assumed that all TRU discharged are recovered and 5% of the rare-earth fission products are carried over with the recycled TRU. A schematic configuration of the ATW core is shown in Figure 5. The detailed core design characteristics of the sodium-cooled ATW can be found in Ref. 9.

Table 5. **Production rates of TRU, ^{99}Tc and ^{129}I in PWR and ATW systems**

Fuel Type	Production rate, kg/Gwth·yr		
	TRU	Tc-99	I-129
PWR (33 GWD/MTU burn-up)	107.9	8.6	2.0
ATW (270 GWD/MTH burn-up)	-369.1	7.1	2.2

Unless special systems dedicated to the LLFP incineration are employed, simultaneous transmutation of both TRU and LLFP (in the appropriate proportion) appears to be highly desirable. In this respect, the LLFP transmutation goal was defined as achieving ^{99}Tc and ^{129}I support ratios equal to the TRU support ratio. In order to estimate these support ratios, the ^{99}Tc, ^{129}I, and TRU production rates in a typical PWR and the ATW system were calculated using the ORIGEN code. [13] A UO_2 fuel composition (typical of a PWR) with 3.2 w/o ^{235}U enrichment was depleted up to 33 GWD/MTU burn-up, and a TRU fuel composition was depleted up to 270 GWD/MTH burn-up, which is the typical fuel discharge burn-up of the ATW system. The results are summarised in Table 5. Using the data in Table 5 and assuming that the PWR and ATW system capacity factors are 80% and 74%, respectively, the TRU support ratio of the 840 MWth ATW system is estimated to be 3.2. Therefore, in order to achieve the same support ratios while accounting for LLFP production in the ATW system, 22.8 kg of ^{99}Tc and 5.6 kg of ^{129}I need to be consumed per year (i.e., 11.4 kg of ^{99}Tc and 2.8 kg of ^{129}I per cycle) in the target assemblies.

Figure 5. **Planar layout of 840 MWT sodium-cooled ATW core (one-sixth core)**

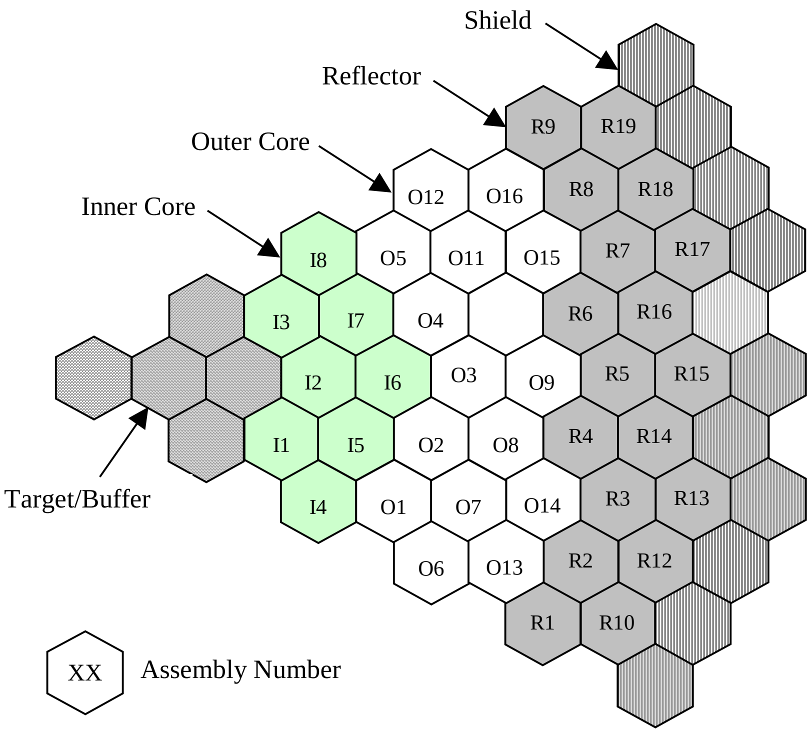

III.2 Heterogeneous transmutation

The heterogeneous transmutation approach was first investigated by focusing on ^{99}Tc transmutation. Two loading options were analysed. In the first option, twelve moderated ^{99}Tc target assemblies were loaded into positions R4 and R6 of the reflector (see Figure 5) and their symmetric counterparts. In the second option, six target assemblies were loaded in the O3 position within the core and its symmetric counterparts.

In the reflector loading case, the R4 and R6 positions were selected since they have higher flux levels than the other reflector positions. The moderated ^{99}Tc target assembly with the ^{99}Tc thermal neutron filter was used; the 28 target pins at the interface between the fuel and target assemblies are composed of the annular ^{99}Tc target only without the moderator, and the other target pins are composed of the annular ^{99}Tc target and ZrH_2 moderator with a 60% moderator volume fraction. The number of target assemblies was determined such that the ^{99}Tc transmutation rate in the target assemblies is roughly 11 kg/cycle.

In the case of the core interior loading, the location of the target assembly should be determined in such a way that a high transmutation rate can be achieved while preserving the source multiplication. For example, although the target assembly loaded in the innermost fuel ring near the spallation target produces the highest ^{99}Tc transmutation rate due to the flux level being highest, it reduces the source multiplication efficiency significantly by directly absorbing the source neutrons. In this study, the O3 location was selected as a compromise between the flux level and the negative impact on the source multiplication. To reduce the local power peaking, solid cylindrical ^{99}Tc pins were loaded in the two outermost rings of the target assembly, and the moderator volume fraction of the internal target pins was increased to 70% to balance the transmutation rate.

By loading the ^{99}Tc target assemblies as discussed above, REBUS-3 equilibrium cycle analyses were performed without modeling the recycle of the target assemblies, since only the fuel constituents can be recycled in the current REBUS-3 equilibrium cycle model. For the target assemblies which are not recycled, these calculations provide only cycle burn-ups. Therefore, using these target cycle burn-ups, the ^{99}Tc discharge burn-ups were estimated for the expected target irradiation time. Assuming that the fractional LLFP cycle burn-up (i.e., the transmuted fraction of the target mass at the beginning of each cycle) is constant, the ^{99}Tc discharge burn-up B_d^{FP} can be determined as:

$$B_d^{FP} = 100 \times [1 - (1 - B_c^{FP})^n],\ \%$$

where B_c^{FP} is the fractional cycle burn-up of an LLFP in the first irradiation cycle and n is the total number of irradiation cycles. In reality, this fractional target cycle burn-up is expected to increase slowly with the irradiation cycle; the flux level of the target assembly would increase slightly due to the significantly smaller capture cross sections of product isotopes of target transmutation (see Section II.2), whereas the capture cross sections of target isotopes remain almost constant. Therefore, the discharge burn-up calculated in this way provides a conservative estimate of the LLFP burn-up.

The lifetime of the moderated target assembly would be determined primarily by the fast-neutron irradiation damage to the cladding (fast fluence limit) and the irradiation damage to the moderator. In this study, because of lack of available data on the long-term irradiation behaviour of ZrH_2, the irradiation time of the ^{99}Tc target assembly was determined based on the fast fluence limit of HT-9 cladding (~4×10^{23} n/cm^2). From the REBUS-3 equilibrium cycle analysis, it was found that for both loading options, the ^{99}Tc target assembly could be irradiated for 14 consecutive fuel cycles (5.2 year) within the fast fluence limit. Based on the world-wide operation histories of TRIGA reactors in which

ZrH_2 moderator is incorporated with enriched uranium metal in the fuel elements, it is expected that the ZrH_2 disintegration would not be a main obstacle to achieving this irradiation time. Therefore, the ^{99}Tc discharge burn-up was evaluated for a 14-cycle irradiation time.

Table 6. **Transmutation performance parameters of heterogeneous ^{99}Tc loading options in equilibrium cycle ATW core**

Parameter		Tc assembly location	
		Core	Reflector
Tc-99 transmutation rate over 14 cycles (1890 EFPDs)	Initial loading, kg	303.8	387.8
	Average burnup, %/cycle	3.00 (3.82*)	2.43 (2.93*)
	Average burnup, kg/cycle	9.12 (11.6*)	9.43 (11.4*)
	Discharge burnup, a/o	42.0	34.1
TRU fuel	Inventory, kg	3,072	2,910
	Discharge burnup, a/o	25.6	26.9
Local power peaking in seven-assembly model		1.39	1.43
Initial total flux in Tc target assembly, n/cm^2sec		2.57E+15	1.33E+15
Peak discharge fast fluence in Tc assembly, n/cm^2		3.92E+23	2.38E+23

* Tc-99 cycle burnup in the first irradiation cycle

The resulting ^{99}Tc transmutation rates and selected core performance parameters are presented in Table 6. It can be observed that the two ^{99}Tc transmutation options could meet the required ^{99}Tc supporting ratio by slightly increasing the ^{99}Tc loading. The in-core burning of ^{99}Tc provides a 24% higher relative transmutation rate than the reflector loading case, due to the higher flux level. Although the flux level is almost doubled in the in-core burning case, the increase in the transmutation rate is not proportionally high. This is attributed to the fact that the effective capture cross section of ^{99}Tc is significantly smaller in the in-core case due to the harder neutron spectrum than in the reflector loading. For the in-core loading, the 42 a/o discharge burn-up might be a maximum value due to the fluence limit. However, in the case of the reflector loading, the target discharge burn-up could be significantly increased with a longer irradiation time: the peak fast fluence is only about 60% of the limit.

As shown in Table 6, the in-core burning option requires a slightly higher TRU fuel inventory than the reflector loading case, and hence results in 5% lower fuel discharge burn-up, although the absolute ^{99}Tc transmutation rate (kg/cycle) is comparable in both cases. This is due to the relatively large neutron leakage in the ATW core. The in-core burning requires additional neutrons to compensate the neutrons absorbed by ^{99}Tc target, whereas the ^{99}Tc target in the reflector is mainly transmuted by the neutrons leaking out of the core. This indicates that the ^{99}Tc burning in the reflector is preferable to the in-core burning from the neutron economy point of view.

As discussed above, the local power peaking factor of 1.43 for the reflector loading case is considered to be acceptable since the power densities in the core peripheral fuel assemblies are much lower than the core average power density (240 W/cc). However, the in-core burning option increases the average core power density to 252 W/cc because of the reduced number of fuel assemblies. This increased power density makes the local power peaking problem worse, and hence the local power peaking factor of 1.39 might not be acceptable. In order to reduce the power peaking, the thermal neutron leakage should be further reduced by decreasing the moderator volume and/or by increasing the number of peripheral filter pins. This modification would reduce the ^{99}Tc transmutation rate. Alternatively, the power peaking problem can be mitigated by reducing the TRU fuel enrichment in the adjacent fuel assemblies. However, this makes the core design and fuel management more complicated and increases the fuel fabrication cost.

The in-core LLFP transmutation has another potential problem from the safety point of view. In general, the reactivity effect of the LLFP target assembly is quite large when it is loaded in the middle of core. As a result, an accident involving the loss of target materials could inject a large amount of reactivity into the core. Meanwhile, the corresponding reactivity of an LLFP assembly in the reflector zone is much smaller, compared with the in-core case. Consequently, any melting or ejection of an LLFP assembly from the reflector would be a more benign.

Transmutation of LLFP in the ATW reflector displaces steel reflectors, while still providing adequate shielding. Therefore, the LLFP burning in the reflector reduces the generation of steel activation products. This is viewed as another advantage of the reflector loading option over the in-core loading one.

III.3 Homogeneous transmutation

Another option for ^{99}Tc transmutation is direct mixing of ^{99}Tc with fuel. In this so-called homogeneous transmutation option, the high neutron flux in the fast reactor core can effectively be used without adverse self-shielding of ^{99}Tc. One disadvantage of this approach is that the effective capture cross section is small due to the hard neutron spectrum. This option is not considered for iodine transmutation because of the xenon gas production, which would adversely affect the fuel performance.

As shown in Figure 5, the sodium-cooled ATW core employs two TRU enrichment zones (low-enrichment inner zone and high-enrichment outer zone) to flatten the radial power distribution. Thus, if ^{99}Tc is loaded uniformly in the whole core, the required outer zone TRU enrichment would become too high. On the other hand, since the flux level of the ATW core is significantly higher in the inner zone than in the outer region, the ^{99}Tc would be more effectively burned in the inner zone; however, too much loading of ^{99}Tc in the inner zone may seriously reduce the multiplication efficiency of the external neutron source. Taking these factors into account, ^{99}Tc was loaded in such a way that the loading density of ^{99}Tc in the inner core is about twice that of the outer zone. In addition, ^{99}Tc was not loaded in the outermost fuel ring to enhance the burn-up of ^{99}Tc and flatten the radial power distribution.

The ^{99}Tc transmutation performance of ATW for the homogeneous loading option was assessed by the REBUS-3 equilibrium cycle analyses with target material recycle modelled. Seven and eight batch fuel management schemes were utilised for the inner and outer zones, respectively. The results are summarised in Table 7. As discussed before, the ^{99}Tc discharge burn-up decreases as the ^{99}Tc loading increases, while the absolute transmutation rate (kg/cycle) increases with the ^{99}Tc loading. By comparing Tables 6 and 7, it can be observed that for the same ^{99}Tc loading, the homogeneous loading option results in transmutation performance inferior to the heterogeneous loading options. The significantly lower ^{99}Tc discharge burn-up is mainly due to the short irradiation time: 945 days in the inner core and 1 080 days in the outer core. The lower cycle burn-up is caused by the small capture cross-section resulting from the hard neutron spectrum. The homogeneous loading option also requires a larger TRU fuel inventory than the heterogeneous loading in the reflector, even though its ^{99}Tc support ratio is still significantly lower.

Table 7. **Transmutation performance parameters of homogeneous ^{99}Tc loading option in equilibrium cycle ATW core**

Initial ^{99}Tc inventory, kg	^{99}Tc transmutation rate			Initial fuel inventory, kg	Fuel discharge burnup, a/o
	%/cycle	kg/cycle	Discharge burnup, a/o		
0	–	–	–	2 744	28.3
45	2.90	1.30	19.8	2 775	28.0
89	2.81	2.50	19.1	2 813	27.7
176	2.68	4.72	18.2	2 878	27.2
343	2.42	8.33	16.5	3 014	26.1

III.4 Simultaneous transmutation of ^{99}Tc and ^{129}I

In order to achieve support ratios for ^{99}Tc and ^{129}I equal to the TRU support ratio, the simultaneous transmutation of both ^{99}Tc and ^{129}I in the ATW core was studied. Based on the above loading option studies, it was decided to load moderated LLFP target assemblies in the reflector region. The moderated LLFP target assembly designs with the ^{99}Tc thermal neutron filter discussed in Section II.2 were used. The reflector positions which have relatively higher flux levels were selected for LLFP assembly loading. Twelve ^{129}I target assemblies were loaded into the R4 and R6 positions and their symmetric counterparts (see Figure 5) which have the highest flux levels in the reflector region, and twelve ^{99}Tc target assemblies were loaded into the R2 and R8 positions and their symmetric counterparts which have the next highest flux levels.

The resulting LLFP transmutation rates showed that the ^{99}Tc transmutation rate is sufficient to meet the support ratio goal but the ^{129}I transmutation rate is not. Therefore, to increase the absolute transmutation of ^{129}I and to enhance the LLFP discharge burn-ups at the same time, the above "standard" assembly designs were further optimised. As discussed in Section II, the target discharge burn-up increases monotonically as the moderator volume fraction increase (i.e., as the target volume fraction decreases). On the other hand, for a moderator volume fraction near that of the standard design (60%), the absolute transmutation rates decreases as the target loading decreases. As a result, in order to increase the discharge burn-up while satisfying the support ratio goal, it is necessary to increase the moderator volume while maintaining the ^{99}Tc loading and increasing the ^{129}I loading. The only possible way to accomplish this without introducing additional target assemblies is to increase the total target pin volume by reducing the coolant volume.

Accordingly, modified assembly designs were developed by reducing the pitch-to-diameter (P/D) ratio of target pins to its minimum value of 1.0, keeping the same number of target pins per assembly. In these modified designs, the target pin diameter was increased from the reference value of 0.63 cm to 0.89 cm with the same clad thickness. The moderator volume fraction within each ^{99}Tc target pin was increased to 72% from 60% in order to maintain the ^{99}Tc loading, but it was increased only to 65% for ^{129}I target pins since the ^{129}I loading needed to be increased. (The ^{129}I loading per assembly was increased by ~18% relative to the standard design.) Although the moderator volume fractions inside target pins are not increased much relative to the standard designs, the moderator volume fraction of the assembly is significantly increased due to the reduced coolant volume fraction, and hence the neutron spectrum is much softer in these modified designs. Additionally, in the modified ^{99}Tc target assembly, the central void of the annular ^{99}Tc thermal neutron filter was filled with HT-9 in order to mitigate increased power peaking from the enhanced moderation by increasing the parasitic absorption.

The resulting LLFP transmutation rates and selected core performance parameters are presented in Table 8. It can be seen that the transmutation rates obtained with the modified LLFP assembly designs are high enough to meet the support ratio goals for both ^{99}Tc and ^{129}I. The modified assembly design increases the absolute and relative transmutation rates of ^{129}I by ~60% and ~18%, respectively, but it increases the ^{99}Tc transmutation rates only by ~4%. This is due to the fact that the moderator is more effective in increasing the effective capture cross section of ^{129}I than that of ^{99}Tc as discussed in Section II. It is noteworthy that the total flux levels in the modified design are significantly lower than those in the standard design, due to the softened neutron spectrum. This reduced flux largely offsets the increase in capture cross sections, particularly for ^{99}Tc. When the modified LLFP designs are used, the TRU inventory is increased by about 1.9% mainly because of increased ^{129}I loading. The local power peaking factors obtained from the seven-assembly model VIM calculations are less than 1.45, and these values are considered to be acceptable since the highest average power density (177 W/cc) in the fuel assemblies adjacent to target assemblies is only ~74% of the core average power density (240 W/cc) as shown in Figure 6.

Table 8. **Transmutation performance parameters of simultaneous loading of ^{99}Tc and ^{129}I in reflector region of equilibrium cycle ATW core**

Parameter			**LLFP assembly**	
			Standard (P/D=1.1969)	P/D=1.0
LLFP transmutation rate over 14 cycles (1890 EFPDs)	Initial loading, kg	Tc-99	620.1	620.2
		I-129	83.1	112.6
	Average %/cycle	Tc-99	1.96 (2.27*)	2.05 (2.38*)
		I-129	2.26 (2.68*)	2.65 (3.26*)
	Average kg/cycle	Tc-99	12.2 (14.1*)	12.7 (14.8*)
		I-129	1.88 (2.23*)	2.99 (3.67*)
	Discharge burnup, a/o	Tc-99	27.5	28.6
		I-129	31.6	37.1
TRU fuel	Inventory, kg		2,984	3,040
	Discharge burnup, a/o		26.3	25.9
Local power peaking in seven-assembly model		Tc-99 target	1.43	1.45
		I-129 target	1.40	1.44 (1.88**)
Initial total flux in LLFP assembly, n/cm^{2}sec		Tc-99 target	9.09E+14	6.73E+14
		I-129 target	1.31E+15	1.06E+15
Peak discharge fast fluence in LLFP assembly, n/cm^2		Tc-99 target	1.82E+23	1.68E+23
		I-129 target	2.38E+23	2.24E+23

* LLFP cycle burnup in the first irradiation cycle

** HT-9 rods are used instead of Tc-99 rod as the thermal neutron filter

Mainly the neutrons leaking out of the core transmute the LLFP target assemblies loaded in the reflector. As a result, the impact on the core performance parameters was generally minor. Compared to the base design without any LLFP loading, the loading of modified LLFP assemblies in the reflector region increases the TRU inventory only by ~10%, and reduced the TRU discharge burn-up only by ~8%. This increased inventory reduces the burn-up reactivity swing slightly. The peak power density still occurs within the core (near the interface between inner and outer cores in Figure 5), and the global peaking factor is basically the same as the base design.

In the modified LLFP assembly designs, the pitch-to-diameter ratio of target pins is 1.0, and hence the coolant flow area is reduced by a factor of ~4 relative to the ATW fuel assembly. Thus, adequate cooling of target pins might be a concern. However, as shown in Figure 6, the power densities in the LLFP target assemblies are less than 10% of the core average power density (240W/cc). Therefore, considering the excellent thermal properties of sodium coolant, it is believed that the LLFP target pins can be adequately cooled.

Figure 6. **Assembly average power densities (W/cc) of equilibrium cycle ATW with ^{99}Tc/^{129}I target assemblies (P/D=1.0) in the reflector region**

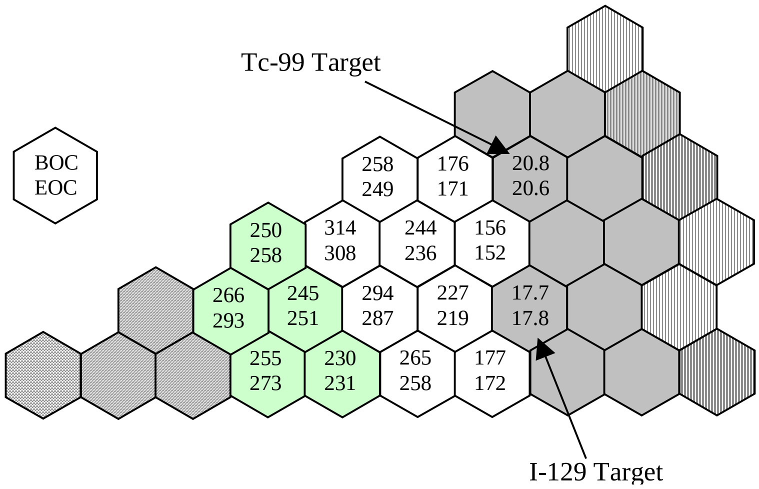

IV. Conclusions and future works

In order to devise an optimal strategy for transmuting LLFPs in fast systems, design optimisation studies have been performed for an 840 MWth sodium-cooled ATW system. Using ^{99}Tc metal and CaI_2 target forms and ZrH_2 moderator, assembly design optimisation studies were first done to maximise the LLFP transmutation performance and to mitigate the local power peaking problem in neighbouring fuel assemblies caused by moderation in the target assembly. Based on these studies, various LLFP loading options in the ATW core were evaluated by performing full core neutronics and depletion calculations.

From the design optimisation studies on the moderated LLFP assemblies, the following conclusions are drawn:

- The transmutation rates of ^{99}Tc and ^{129}I are significantly enhanced by employing ZrH_2 moderator. In order to minimise the self-shielding effects, the target nuclides need to be loaded as dilutely as possible. The annular target configuration filled with the moderator reduces the self-shielding effects and increases the effective capture cross sections relative to the separate target and moderator pin configuration.

- There exists an optimal moderator volume fraction to maximise the absolute transmutation rate. However, the LLFP discharge burn-up increases monotonically with the moderator volume fraction (i.e., as the LLFP loading decreases). For a fixed LLFP loading, the moderator volume needs to be maximised to increase the transmutation rate.

- The local power peaking in the neighbouring fuel assemblies can be effectively mitigated by employing ^{99}Tc target pins at the interface between fuel and target assemblies.

In the sodium-cooled ATW system, the heterogeneous loading of LLFP target material in special moderated assemblies enables higher LLFP discharge burn-up than the homogeneous mixing of target and fuel. Among various heterogeneous loading options, loading of LLFP in the reflector region seems to be the best option from the neutron economy and safety perspectives. This option provides sufficient transmutation rates to meet the goal of achieving a support ratio for LLFP equal to that of TRU. With a simultaneous loading of twelve ^{99}Tc and twelve ^{129}I target assemblies in the reflector region, ^{99}Tc and ^{129}I can be consumed with a support ratio equal to the TRU support ratio (~3.2) at the cost of a 10% increase in fuel inventory. Discharge burn-ups of ~29% and ~37% are achieved for ^{99}Tc and ^{129}I target assemblies with a ~5-year irradiation period.

The ^{99}Tc discharge burn-up is somewhat lower than that of ^{129}I because of the lower flux level in the ^{99}Tc target assembly. By employing more ^{99}Tc target assemblies with correspondingly reduced ^{99}Tc loading per assembly, the ^{99}Tc discharge burn-up can be increased while maintaining the support ratio. However, this approach would increase the target fabrication and recycle costs.

For the realisation of the high targeted ^{129}I discharge burn-up, a sufficiently long gas plenum must be provided to accommodate xenon gas produced by iodine transmutation. In the modified ^{129}I target case, the gas plenum needs to be very long (about 170 cm) in order to keep the xenon pressure below 100 atm under the conservative assumption that all xenon gas is released from the target material to the gas plenum. By increasing the number of ^{129}I target assemblies with reduced iodine loading per assembly, the xenon pressure build-up can be mitigated without reducing the support ratio. In this case, the relative transmutation rate of ^{129}I would be enhanced because of the increased moderator volume fraction, but the greater number of target assemblies would increase cost.

REFERENCES

[1] J.L. Kloosterman and J.M. Li (1995), *Transmutation of ^{99}Tc in Fission Reactors*, Proc. 3rd Int. Information Exchange Mtg. Actinide and Fission Product Partitioning and Transmutation, Cadarache, France, NEA/P&T Report No. 13, p. 285, OECD.

[2] K.D. Dobbin (1991), *Transmutation of LWR High-level Waste in LMRs*, ANS Transaction, 64, 122.

[3] T. Wakabayashi and N. Higano (1998), *Study on MA and Fission Product Transmutation in Fast Reactors*, Progress in Nuclear Energy, 32, 555.

[4] H. Golfier *et al.* (1999), *Parametrical Analysis of ^{99}Tc and ^{129}I Transmutation in Reactor*, Proc. Int. Conference on Future Nuclear Systems GLOBAL '99, Wyoming USA.

[5] W.S. Park *et al.* (2002), *A Design Study of ^{99}Tc and ^{129}I Transmutation in the HYPER System*, accepted for publication in Nuclear Science and Engineering.

[6] D.W. Wootan, *et al.* (1991), *Irradiation Test of ^{99}Tc and ^{129}I Transmutation in the Fast Flux Test Facility*, ANS Trans. 64, 125.

[7] R.J.M. Kornings *et al.* (1997), *Transmutation of Technetium and Iodine-irradiation Tests in the Frame of the EFTTRA Cooperation*, Nuclear Technology, 117, 293.

[8] A. Conti, J.P Ottaviani *et al.* (1999), *Long-lived Fission Product Transmutation Studies*, Proc. Int. Conference on Future Nuclear Systems GLOBAL '99, Wyoming USA.

[9] R.N. Hill *et al.* (2000), *Physics Studies of a Sodium Cooled ATW Design*, Proceedings of the IAEA Technical Committee Meeting on Core Physics and Engineering Aspects of Emerging Nuclear Energy Systems for Energy Generation and Transmutation, Argonne National Laboratory, Nov. 28-Dec. 1.

[10] R.N. Blomquist, (1980) *VIM-A Continuous Energy Monte Carlo Code at ANL*, Proceedings of a Seminar-Workshop on a Review of the Theory and Application of Monte Carlo Methods, ORNL/RSIC-44, April 21-23.

[11] B.J. Toppel (1983), *A User's Guide to the REBUS-3 Fuel Cycle Analysis Capability*, ANL-83-2, Argonne National Laboratory.

[12] H. Henryson II, B.J. Toppel and C.G. Stenberg (1976), *MC^2-2: A Code to Calculate Fast Neutron Spectra and Multigroup Cross-sections*, ANL-8144, Argonne National Laboratory.

[13] A.G. Croff (1980), *A User's Manual for the ORIGEN2 Computer Code*, ORNL/TM-7175, Oak Ridge National Laboratory.